Proceedings of the ASME 2010 3rd Joint US-European Fluids Engineering Summer Meeting and 8th International Conference on Nanochannels, Microchannels, and Minichannels
FEDSM-ICNMM2010
August 1-5, 2010, Montreal, Canada

FEDSM-ICNMM2010-30680

NUMERICAL SIMULATION OF FLOW AROUND A GENERIC PICKUP WITH ISIS-CFD

Emmanuel Guilmineau
Laboratoire de Mécanique des Fluides, CNRS UMR 6598
Ecole Centrale de Nantes
BP 92101, 44321 Nantes Cedex 3, France
Email: Emmanuel.Guilmineau@ec-nantes.fr

ABSTRACT

Computational Fluid Dynamics (CFD) is used to simulate the flow over a pickup truck. The flow solver used is ISIS-CFD developed by the CFD Department of the Fluid Mechanics Laboratory of Ecole Centrale de Nantes. CFD simulations are carried out with the Explicit Algebraic Reynolds Stress Model (EARSM) turbulence model and the Detached Eddy Simulation (DES). The focus of the simulation is to assess the capabilities of ISIS-CFD for vehicle aerodynamic development for pickup trucks. Detailed comparisons are made between the CFD simulations and the existing experiments for a generic pickup truck. The comparisons between the simulation results and the time-averaged measurements reveals that the CFD calculations are able to track the flow trends.

INTRODUCTION

The external aerodynamics of a car determines many relevant aspects of an automobile such as stability, comfort and fuel consumption at high cruising speed [1]. The aerodynamics of road vehicles has frequently been studied in simplified geometries to separate the effect of various components on aerodynamic drag and on near wake flow dynamics. Several simple generic reference models have been proposed in the past to experimentally investigate the automotive aerodynamics and isolate relevant flow phenomena [2]. The most popular simple model proposed for such investigations is Ahmed body [3]. The proportions of modern vehicles are not the same as those of models. And the most significant models do not cover the proportions of vehicles sold in North America. Recently, a joint computational-experimental benchmark study was realized for a pickup by Al-Garni *et al* [4] and Lokhande *et al* [5]. In this study, the authors conduct an investigation of flow past a generic pickup truck that represents a realistic automotive bluff shape.

The aerodynamics of pickup truck is more complex than other road vehicle. Due to the presence of the bed of the pickup truck and the interactions of the wake flow leaving the pickup truck cab with the bed, the flow around a pickup truck is intrinsically complex. And the understanding of the flow field over pickup trucks is a lot less than the understanding over sedans or SUVs for which a lot of effort have spent on the aerodynamics. A recent experimental investigation of the flow in the near wake of a pickup truck model has been conducted [4]. In this study, instantaneous flow field over a 1/12-scale generic pickup truck was measured using the particle imaging velocimetry (PIV) technique. The measurements provided the instantaneous velocity field at certain planes in the bed and the wake region. The pressure distributions on the pickup truck surfaces were also measured in the experiments. The CFD simulations for flow over pickup truck follows the same tendency than the experiments for this geometry. Numerical computations have been performed using the commercial CFD tools [5]. Transient formulations were used in order to capture the unsteadiness of the flow field. In this case, a steady state solution is first obtained. Then, this solution is used to initialize the transient simulation with a time step of 0.002 s. When the solution reaches dynamic stability, the time step is gradually reduced to 0.0003 s. The flow structures from the CFD simulations were found to be similar to those observed

in experiments. More recently, another numerical study [6], with a steady state formulation rather than an unsteady formulation, showed this formulation capture the structure of the flow field around a pickup truck. Further more, CFD results also given the same direction of change for the aerodynamics drag variations due to the change of vehicle geometric configurations, such as the change from the short bed to long bed. Another comparison [7] between a conventional body-fitted and the Lattice Boltzmann CFD methods has been performed for the prediction of the flow around a generic pickup truck. This study showed that the CFD codes were not able to predict correctly the drag. Indeed, the CFD codes used predicted the drag within 12% of the measured value.

The present CFD simulation are based on the using of the ISIS-CFD solver, which is developed in the CFD group of the Fluid Mechanics laboratory of the Ecole Centrale de Nantes. This solver, included in the computational suite FINE™/Marine, is used to capture the unsteadiness of the flow field around a generic pickup truck model. The objective of this study is to assess the capabilities of this flow solver when it is applied to flow around pickup truck. In automotive field, this solver is only validated for simplified car models [8, 9]. However, this flow solver has been validated for complex geometries and in particular in hydrodynamics field [10, 11].

In this paper, the aerodynamic characteristics of a pickup truck are study using numerical simulation. To take account the turbulence of the flow, two turbulence models are used. The first model is a Explicit Algebraic Reynolds Stress Model (EARSM) and the second use the Detached Eddy Simulation (DES). These turbulence models are already used to simulate the cross wind effects around a car model [9, 12]. All simulation results are evaluated against experimental data [4].

PICKUP MODEL

The generic extended cab pickup truck model used in the previous study [4,5,7] was used for the present investigation. The model represents a 1:12 scale of the full-scale pickup truck. The model is designed with a smooth underbody, enclosed wheel-wells and without openings for cooling airflow. A schematic view of the pickup truck with the dimensions is depicted in Fig. 1. The length of the model is 0.432 m, the width is 0.152 m, and the height is 0.148 m. The maximum cross section area is 0.0195 m^2. A coordinate system is attached to the front tip of the model in the symmetry plane are shown in Fig. 1.

The inlet velocity, U_{in}, is 30m/s. The Reynolds number, based on the length of the pickup, is Re = 864,000. Instantaneous flow field was measured using the Particle Imaging Velocimetry (PIV) technique. The pressure distribution on the pickup truck surfaces were also measured in the experiments. The experiments were conducted in the wind tunnel at the University of Michigan [4]. This is an open-return suction wind tunnel equiped with glass

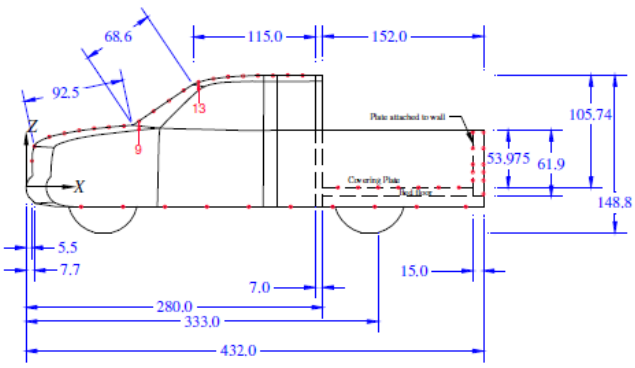

FIGURE 1. SIDE VIEW FOR THE PICKUP TRUCK (DIMENSIONS ARE IN MM).

side and bottom test section walls for optical access. The tunnel has 140 mm filets on the edges opposing to the floor. These filets are also take into account in the simulations.

FLOW SOLVER

The ISIS-CFD flow solver, developed by the EMN (Equipe Modélisation Numérique) of the Fluid Mechanics Laboratory of Ecole Centrale de Nantes, uses the incompressible unsteady Reynolds-averaged Navier Stokes equations (URANSE). The solver is based on a finite volume method to build the spatial discretization of the transport equations. The face-based method is generalized to two-dimensional, or three-dimensional unstructured meshes for which non-overlapping control volumes are bounded by an arbitrary number of constitutive faces. Numerical fluxes are reconstructed on mesh faces by linear extrapolation of integrand from the neighboring cell centers. A centered scheme is used for the diffusion terms, whereas for the convective fluxes, the scheme implemented in the ISIS-CFD code is the Gamma Differencing Scheme (GDS) [13]. Through a Normalized Variable Diagram (NVD) analysis, this scheme enforces local monotonicity and convection boundedness criteria.

The velocity field is obtained from the momentum conservation equations and the pressure field is extracted from the mass conservation constraint, or continuity equation, transformed into a pressure-equation. These non-linear and coupled equations are solved by a segregated SIMPLE-like algorithm. A second-order accurate three-level fully implicit time discretization is used and surface and volume integrals are evaluated using second-order accurate approximation. In the case of turbulent flows, additional transport equations for the modeled variables are discretized and solved using the same principles.

In this study, a quadratic Explicit Algebraic Reynolds Stress Model (EARSM) [14] is used. This model adopts the SSG pressure-strain rate model [15], and solves the BSL k-ω

model [16] to determine the turbulence velocity and length scales. It takes into account the variation of the production-to-dissipation rate ratio. This model can be integrated down to the wall and gives correct log law behaviors in cases without recirculation. The equations of this model are presented in [9].
The DES-SST turbulence model presented by Menter and Kuntz [17] is also used. The idea behind the DES model of Strelets [18] is to switch from the standard k-ω SST of Menter [16] to an LES model in those regions where the turbulent length, L_t, predicted by the k-ω SST model is larger than a local grid spacing. In this case, the length scale used in the computation of the dissipation rate in the equation for the turbulent kinetic energy is replaced by the local grid spacing Δ. The destruction term, that is equal to $\varepsilon = \beta^* \times \omega \times k$ in the k-ω SST model, becomes $\varepsilon = \beta^* \times \omega \times k \times F_{DES}$ in DES where ε is the dissipation rate, Δ is the local grid spacing, β^* is a constant of the k-ω SST model and the function F_{DES} is defined

$$F_{DES} = \max\left(\frac{L_t}{C_{DES}\Delta}, 1\right) \quad (1)$$

where the turbulence length is defined by $L_t = \sqrt{k}/(\beta^* \times \omega)$, $\Delta = \sqrt{\Delta x^2 + \Delta y^2 + \Delta z^2}$ and $C_{DES} = 0.78$.

COMPUTATIONAL DETAILS

The computational domain starts at 2.5×L from the origin in front of the model and extends to 4×L behind the model. This inlet position is widely used, see [5,7]. Even for the Ahmed model, this position is used, see [19,20]. Moreover, in the paper with experimental results, no information is given on the development of the boundary layer. The length of the domain behind the model is lightly short than the previous authors for which the length of the computational domain extends to 5×L. The section of the computational domain is identical to the test section of the wind tunnel used for the corresponding measurements [4]. The cross-section of the tunnel gives a blockage ratio of 5.2%. The mesh is generated using HEXPRESS™, an automatic unstructured mesh generator. This software generates meshes containing only hexaedrals. Computational grid consists from 16.6 million of cells with 804,000 faces to describe the pickup truck. The surface mesh on the pickup is depicted in Fig. 2. A uniform mesh edge length of 1.5 mm is used for an additional box of refinement in the bed of the pickup, see Fig. 3. Figure 4 presents a view of the mesh in a horizontal plane. This mesh is not fine in the wake of the model. This mesh is the first generated and to complete this study, a grid convergence must be carried out.

For the surface of the pickup, we use a no-slip boundary condition. For the walls of the wind tunnel, we use a wall function. This approach, used to take the walls into account, is the same as the approach proposed by Guilmineau and Chometon [9], who

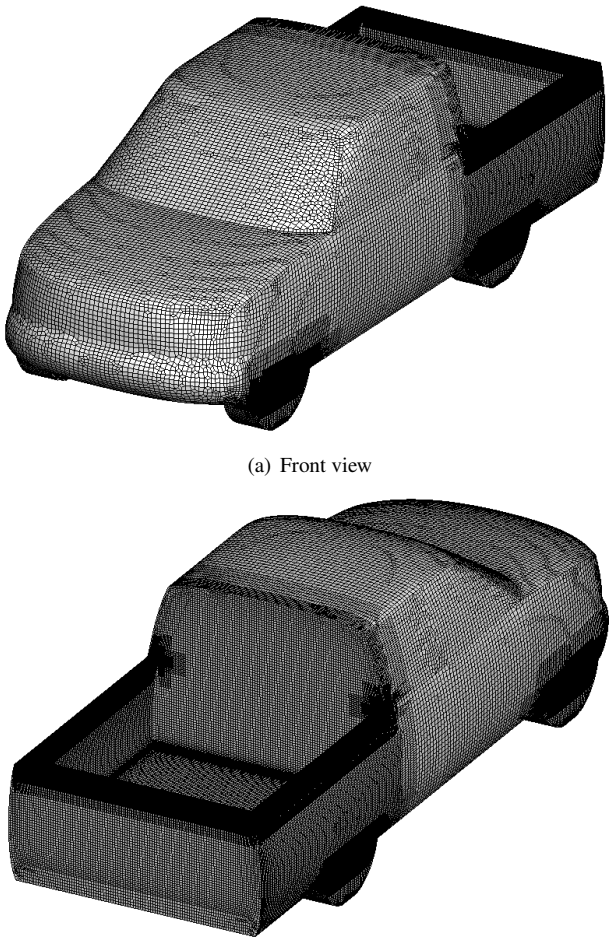

(a) Front view

(b) Back view

FIGURE 2. SURFACE MESH ON THE PICKUP TRUCK.

investigated the crosswind effects around a simplified car model. At the inlet boundary, velocity and turbulent kinetic energy are imposed while at the outlet of the computational domain, the pressure is prescribed.
For the simulation with the EARSM turbulence model, the time step is $\Delta t = 0.0002$ s which corresponds to 72 time steps for one passage of the model at freestream velocity while for the DES the time step is $\Delta t = 0.0001$ s and then 144 time steps for one passage of the model at frestream velocity. Thus, the non-dimensional time is 0.0082 and 0.0041 for the simulation with the EARSM turbulence model and the DES, respectively. As, a implicit formulation is used, the CFL number is not used. These values of time step are close to those used by Lokhande et al [5], which used a time step of 0.0003 s. A maximum of 20 iterations are conducted within each time step to ensure that the continuity and momentum equations were converged till the residuals dropped

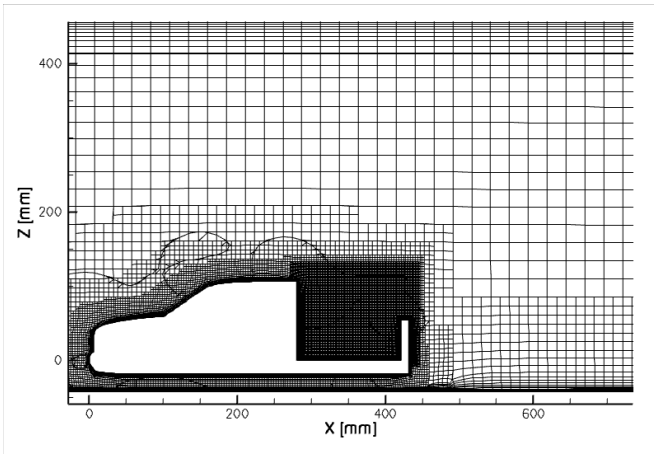

FIGURE 3. MESH IN THE SYMMETRY PLANE.

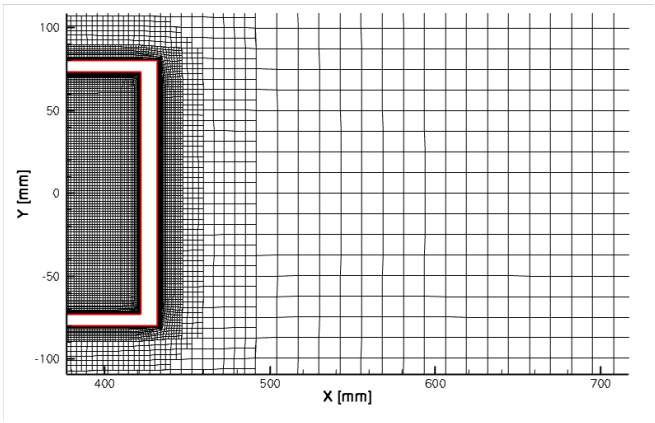

FIGURE 4. MESH IN A HORIZONTAL PLANE.

more than 2 orders. For the DES, only 10 iterations are necessary. The time to obtain an average flow is T = 0.1124 s for the simulation with the EARSM turbulence model and T = 0.3412 s for the DES. The CPU time for the DES is approximatively four times more expensive than the simulation with the EARSM turbulence model.

RESULTS

Following Al-Garni *et al* [4], the local velocity past the vehicle is used as a reference velocity and is defined by:

$$U = U_{in} \frac{A_{tun}}{A_{tun} - A_{veh}} \tag{2}$$

where U_{in} is the tunnel inlet flow velocity (30 m/s), A_{tun} is the tunnel cross-section area (0.2967 m^2) and A_{veh} is the vehicle frontal area (0.0195 m^2). Thus, taking into account the blockage ratio, the pressure coefficient Cp is defined by

$$Cp = \frac{p - p_{ref}}{\frac{1}{2}\rho U^2} \tag{3}$$

where ρ is the air density, and p and p_{ref} are static pressures at the measurement and reference points, respectively. The drag coefficient Cd is given by

$$Cd = \frac{Fx}{\frac{1}{2}\rho U^2 A_{veh}} \tag{4}$$

where Fx is the drag force. The lift coefficient is given by

$$Cl = \frac{Fz}{\frac{1}{2}\rho U^2 A_{veh}} \tag{5}$$

where Fz is the lift force.

Velocity Distribution

Figure 5 shows the streamline comparison in the symmetry plane in the bed of the pickup truck and the near wake region. The overall flow structure predicted by the simulations is seen to match almost exactly with the experimental measurement. A strong recirculating flow region exists behind the cab. The location of the center of the recirculation zone in the bed captured by the simulations is slightly different from that captured by the experiments. Due to the strong downwash, there is no flow reversal in the near wake.

Figure 6 shows the mean velocity field on the left vertical plane (Y = 33 mm). The flow field exhibits a recirculation behind the cab as in the symmetry plane. The shape of this separation is different between the numerical simulation and experiments. Behind the tailgate, a double vortex structure is observed.

The mean flow field in the near wake of the tailgate is shown in Figure 7 at X = 482 mm and in Fig. 8 at X = 550 mm. The numerical results are compared with experiments [21]. These figures presents the mean velocity and vorticity fields in the near wake of the tailgate. The flow is characterized by a pair of strong counter-rotating vortices behind the tailgate. These vortices drag the flow behind the tailgate thus inducing strong downwash at the symmetry plane. In experiments, another weaker pair of vortices appears above the stronger pair of vortices. This second pair of vortices is present in the numerical results but the size and the position are not correct. In the wake, the mesh is not very fine and this can explain why this second pair of vortices is not well predicted. As in experiments, weaker vortex structures originate from the bottom corners of the model. The pair of vortices moves down toward the ground as it travels donwstream as

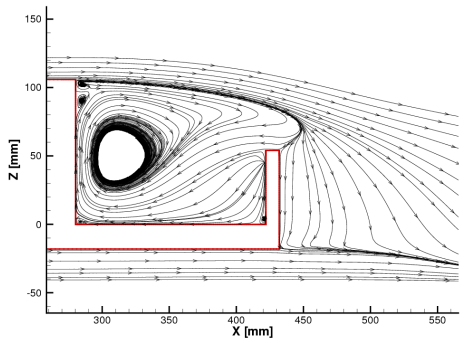

(a) EARSM

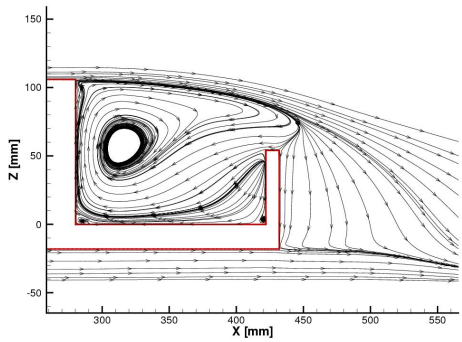

(b) DES-SST

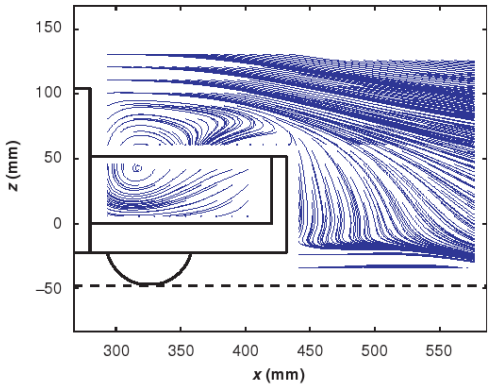

(c) Experiments

FIGURE 5. STREAMLINES IN THE SYMMETRY PLANE.

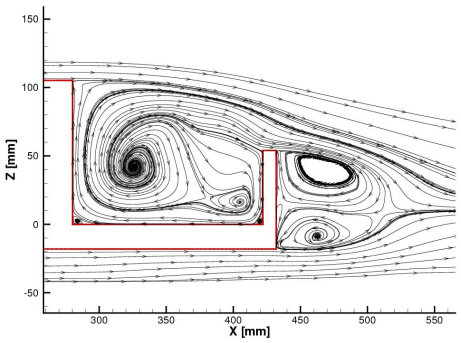

(a) EARSM

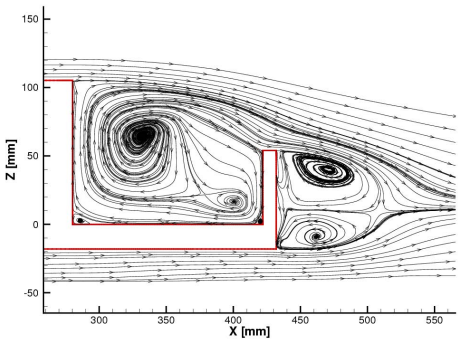

(b) DES-SST

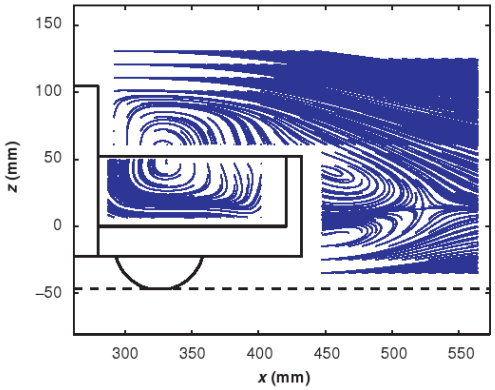

(c) Experiments

FIGURE 6. STREAMLINES IN A VERTICAL PLANE AT Y = 33 MM.

shown in Fig. 8. Between the two positions in the wake, vortices have moved down about 8 mm in the numerical results and about 10 mm in experiments. As these vortices travel downstream, they approach each other.

Additional insights on the three-dimensional flow field around the pickup truck can be extracted from the surface friction lines shown in Figs. 9 and 10, respectively for the EARSM turbulence model and for the DES-SST simulation. No experimental oil-flow visualizations are available, only simulation results are presented. The results are very similar between both numerical results. We can notice the presence of a recirculation area at the base of the windshield. The presence of this recirculation was also found by a numerical simulation with the Spalart-Allmaras model [6]. On the other hand, the same authors [6] did not find this recirculation with another turbulence model. The other flow features, like the attachment line on the front bumper, the under-

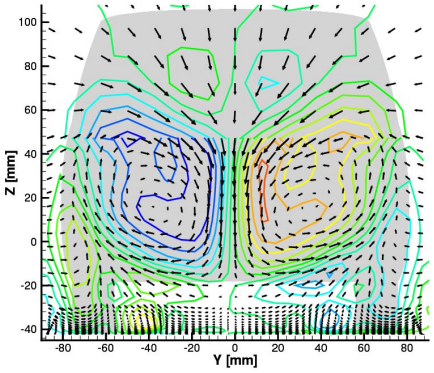

(a) EARSM

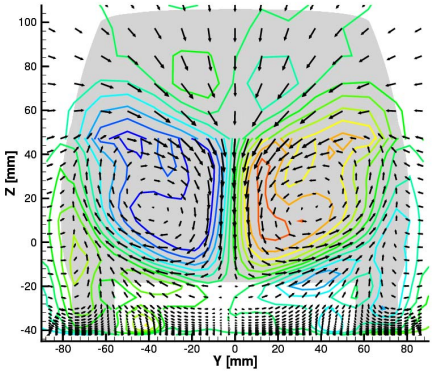

(b) DES-SST

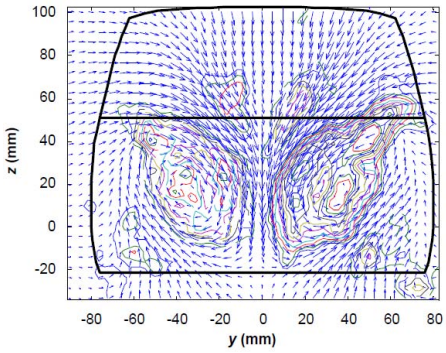

(c) Experiments

FIGURE 7. MEAN VELOCITY AND VORTICITY IN THE NEAR WAKE OF THE TAILGATE AT X = 482 MM.

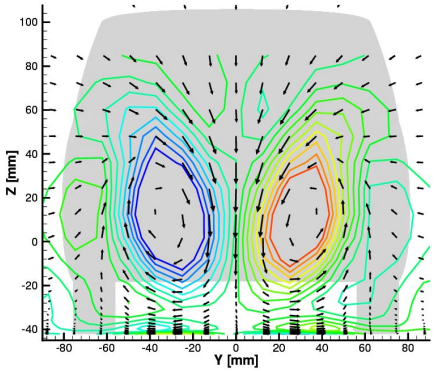

(a) EARSM

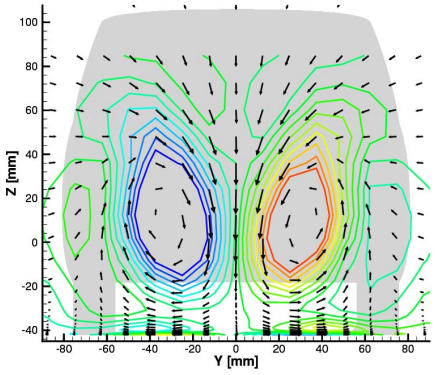

(b) DES-SST

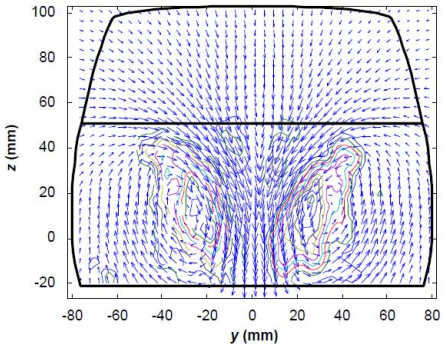

(c) Experiments

FIGURE 8. MEAN VELOCITY AND VORTICITY IN THE NEAR WAKE OF THE TAILGATE AT X = 550 MM.

flow with separation regions behind the wheels, the vortex structure at the tailgate are similar between the two computations and the other simulations [6].

The velocities in the symmetry plane are compared at several X locations, beginning at X = 305 mm immediately behind the cab and extending to X = 540 mm (about 120 mm downstream of the tailgate). The streamwise velocities u/U for the X locations in the bed are shown in Figs. 11 while the streamwise velocities u for the X locations in the wake are shown in Figs. 12. The shape of the velocity profile is captured in the CFD simulations and both simulations given the same results. Inside the bed, the location of zero u-velocity is well captured, suggesting that the size of the recirculation from the experiments and from the CFD are comparable. All u-velocities in Figure 12 are positive, confirm-

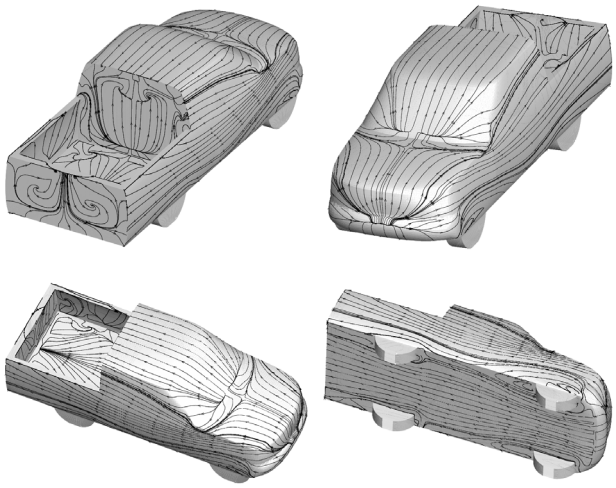

FIGURE 9. FRICTION LINES: EARSM MODEL.

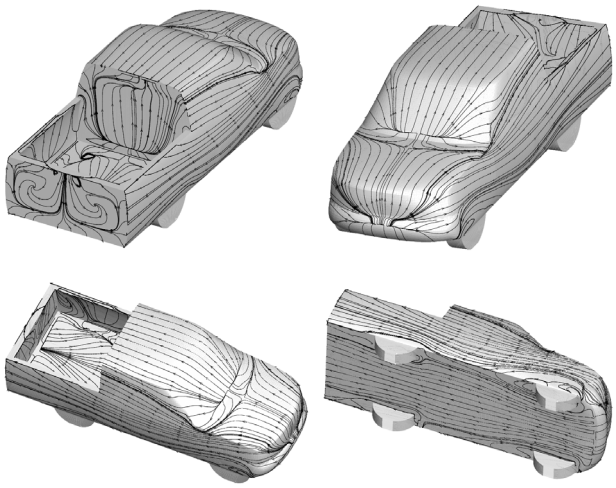

FIGURE 10. FRICTION LINES: DES-SST MODEL.

ing that there is no flow reversal region in the near wake. The evolution of the streamwise velocity shows a reduction of the maximum velocity in the underbody flow when we move away from the body. When we move away from the tailgate, the agreement is less good. At X = 540 mm, the mesh is relatively coarse. This is perhaps an explanation of this disagreement.

The vertical velocities w/U at the same X locations are shown in Figs. 13 and 14 in the bed and in the wake, respectively. The shapes of the vertical velocity distribution are well predicted by the simulations. Minima are slightly underestimated while the extremes are over-estimated. For the flow outside the bed, the results are very similar to those of Yang and Khalighi [6]. The

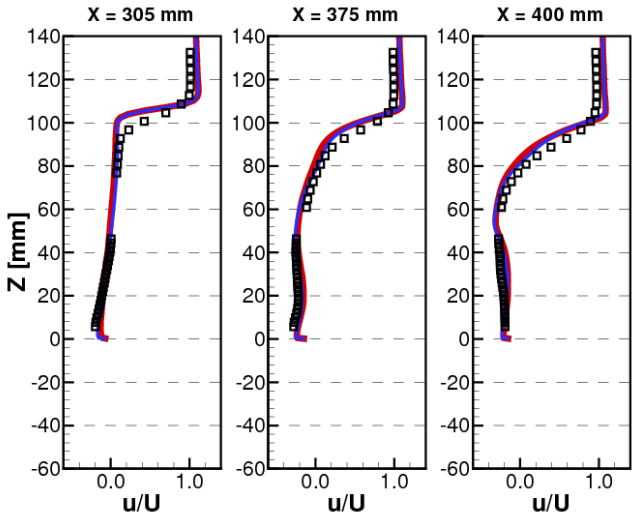

FIGURE 11. STREAMWISE VELOCITY PROFILES ON THE SYMMETRY PLANE IN THE BED (THICK RED LINE = DES-SST, THIN BLUE LINE = EARSM, SYMBOL = EXPERIMENTS).

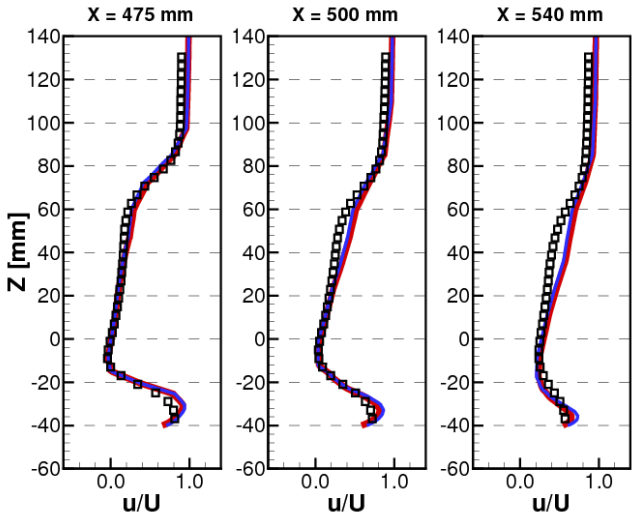

FIGURE 12. STREAMWISE VELOCITY PROFILES ON THE SYMMETRY PLANE IN THE WAKE (THICK RED LINE = DES-SST, THIN BLUE LINE = EARSM, SYMBOL = EXPERIMENTS).

downstream location of the negative maxima is approximately at X $\sim$ 540 mm while in experiments it is at X $\sim$ 500 mm.

Figures 15 and 16 show the normal correlation $\overline{u'^2}/U^2$ in the symmetry plane in the bed and in the wake, respectively. Inside the bed, the normal correlation $\overline{u'^2}/U^2$ increases towards the tailgate. In the cab shear layer, $\overline{u'^2}/U^2$ remains almost constant

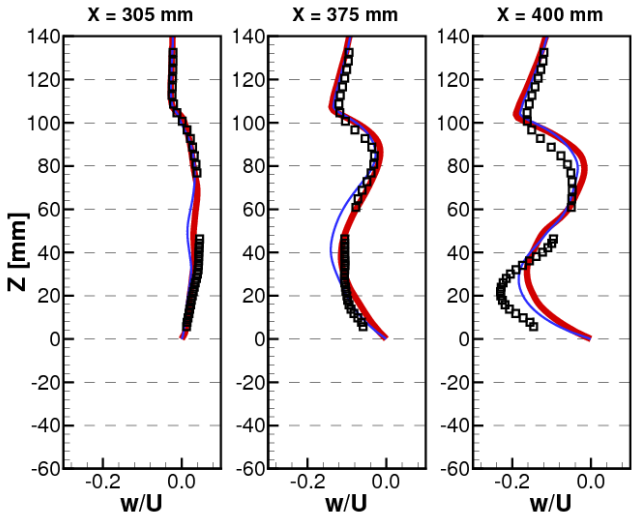

FIGURE 13. VERTICAL VELOCITY PROFILES ON THE SYMMETRY PLANE IN THE BED (THICK RED LINE = DES-SST, THIN BLUE LINE = EARSM, SYMBOL = EXPERIMENTS).

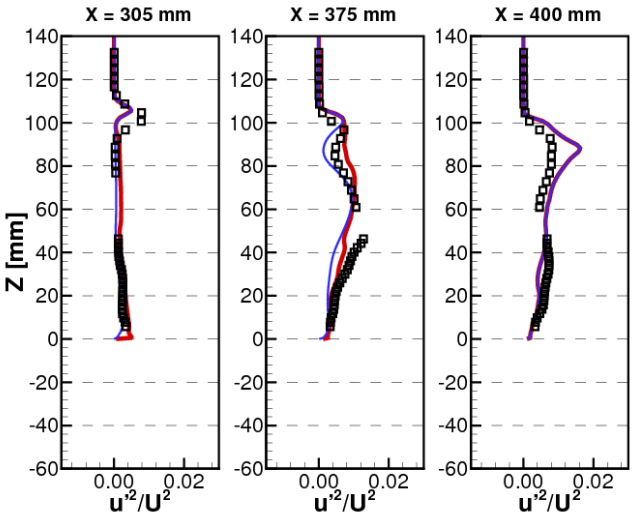

FIGURE 15. NORMAL CORRELATION PROFILES ON THE SYMMETRY PLANE IN THE BED (THICK RED LINE = DES-SST, THIN BLUE LINE = EARSM, SYMBOL = EXPERIMENTS).

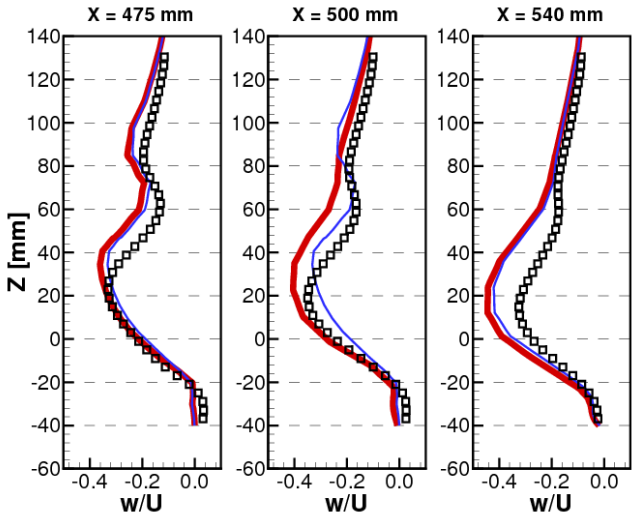

FIGURE 14. VERTICAL VELOCITY PROFILES ON THE SYMMETRY PLANE IN THE WAKE (THICK RED LINE = DES-SST, THIN BLUE LINE = EARSM, SYMBOL = EXPERIMENTS).

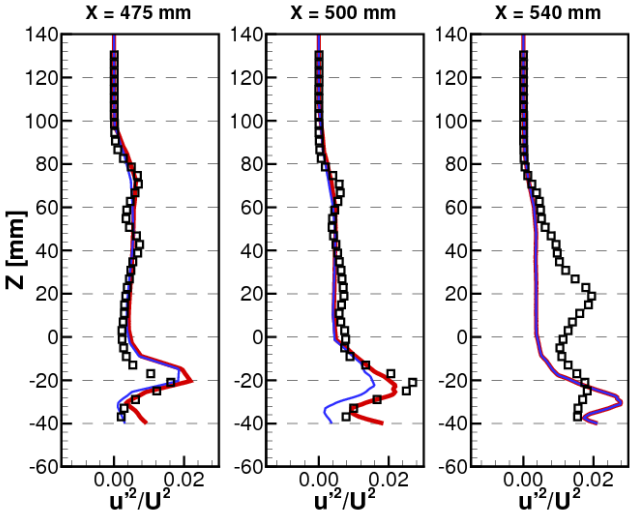

FIGURE 16. NORMAL CORRELATION PROFILES ON THE SYMMETRY PLANE IN THE WAKE (THICK RED LINE = DES-SST, THIN BLUE LINE = EARSM, SYMBOL = EXPERIMENTS).

in the experiments. In the numerical simulations, this value is underpredicted near the cab and overpredicted close to the tailgate. In the wake, the magnitudes of the normal correlation are larger compared to bed flow values. Maximum values are found in the underbody flow shear layer. In experiments, the downstream evolution shows an increase in magnitude up to X = 500 mm, followed by a reduction in magnitude farther downstream. The numerical simulations give an increase until X = 540 mm. And for this position, the agreement is not very good.

The normal correlation in the transverse direction, $\overline{w'^2}/U^2$, is presented in Figure 17 for the bed and in Figure 18 for the wake. In experiments, the maximum normal correlation $\overline{w'^2}/U^2$

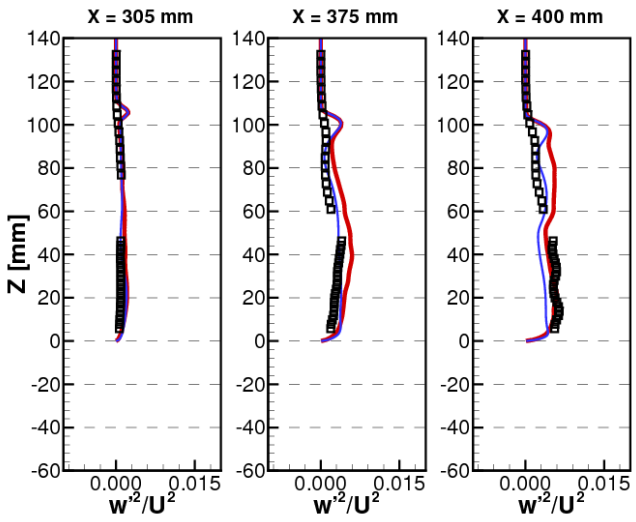

FIGURE 17. NORMAL CORRELATION PROFILES ON THE SYMMETRY PLANE IN THE BED (THICK RED LINE = DES-SST, THIN BLUE LINE = EARSM, SYMBOL = EXPERIMENTS).

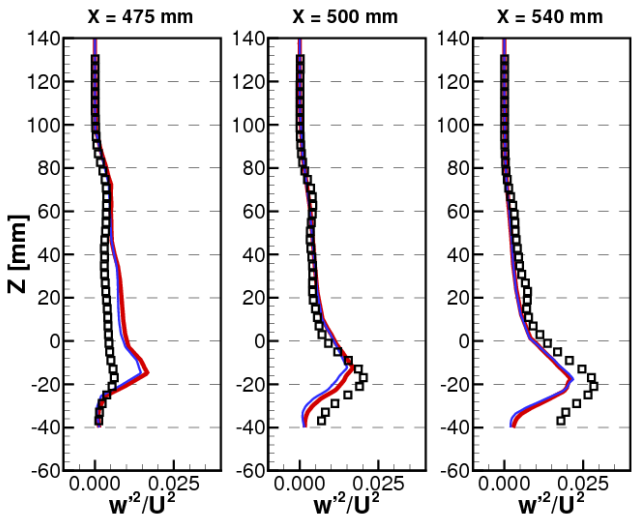

FIGURE 18. NORMAL CORRELATION PROFILES ON THE SYMMETRY PLANE IN THE WAKE (THICK RED LINE = DES-SST, BLUE LINE = EARSM, SYMBOL = EXPERIMENTS).

is larger inside the bed than in the cab shear layer. In the numerical results, the cab shear layer is clearly visible. But as in experiments, this value is about half that of $\overline{u'^2}/U^2$. In the wake, the profiles of $\overline{w'^2}/U^2$ show similar structure as the $\overline{u'^2}/U^2$ correlations. The location of the maximum value is in the underbody flow shear layer.

The shear correlation $\overline{u'w'}/U^2$ in the symmetry plane is presented in Figure 19 for the bed flow and in Figure 20 for the wake flow. The magnitude is smaller in the cab shear layer compared to inside the bed. Maxima are found near the tailgate. In the numerical simulations, the shear correlation in the cab shear layer is more important than in experiments. For the wake flow, as the previous correlations, the maximum value is in the underbody flow shear layer.

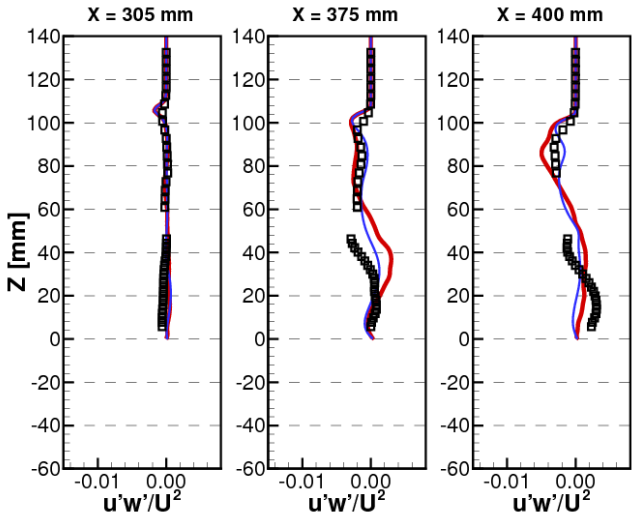

FIGURE 19. SHEAR CORRELATION PROFILES ON THE SYMMETRY PLANE IN THE BED (THICK RED LINE = DES-SST, THIN BLUE LINE = EARSM, SYMBOL = EXPERIMENTS).

Pressure Distribution

Figure 21 shows the measured and the calculated pressure distributions on the hood, windshield, and cab top of the pickup truck in the symmetry plane. CFD predictions and the experiment give the same pattern of pressure distribution. At the front bumper, there is a stagnation point, followed by a rapid drop in pressure due to the transition between the fascia and the hood. On the hood, the flow speed decreases and the pressure increases until the flow reaches the intersection of the hood and the windshield. At this intersection, wen can see a change in the shape of the curve towards X = 100 mm which is due to the presence of the recirculation, as shown Figs. 9 and 10. Then, the pressure decreases over the windshield, and reaches the second low point at the transition between the windshield and the cab top. And then, the pressure recovers on the cab top.

Figure 22 shows the pressure distribution on the cab base in the symmetry plane. Experimentally the pressure coefficient has a minimum value at approximatively the center of the cab base (z

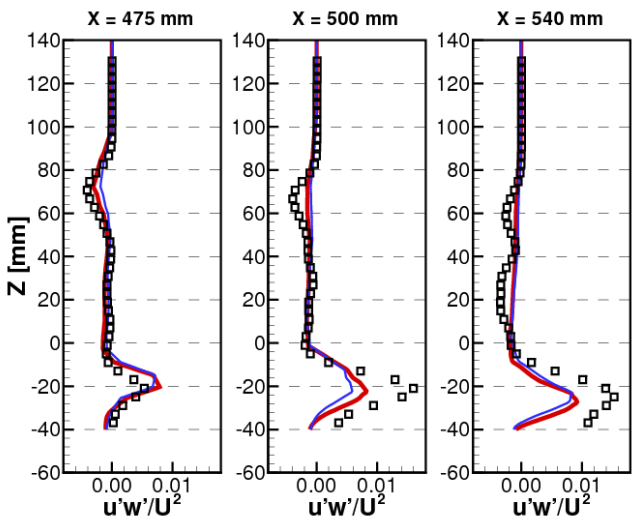

FIGURE 20. SHEAR CORRELATION PROFILES ON THE SYMMETRY PLANE IN THE WAKE (THICK RED LINE = DES-SST, THIN BLUE LINE = EARSM, SYMBOL = EXPERIMENTS).

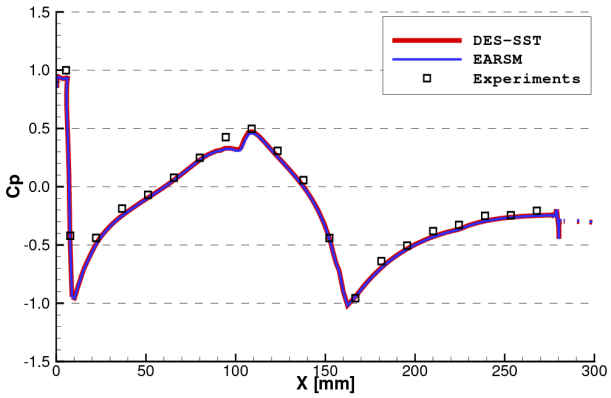

FIGURE 21. PRESSURE DISTRIBUTION ON THE CAB TOP.

$\sim$ 50 mm). The CFD simulations predict the minimum value of Cp at the same position.

Figure 23 shows the pressure on the cab base in a plane parallel to the ground at Z = 50.9 mm. We can see that the pressure distribution is quite flat for the experimental measurements and both numerical results. This remark is also the same for other numerical simulations [6, 7]. This also suggests that the recirculation covers the cab base.

The pressure distribution on the bed floor is shown in Fig. 24. A recirculating flow region is established in the truck bed with the stagnation points at the front and the rear ends of the bed. The simulations correctly predict the higher values for Cp.

The pressure distributions on both sides of the tailgate are shown

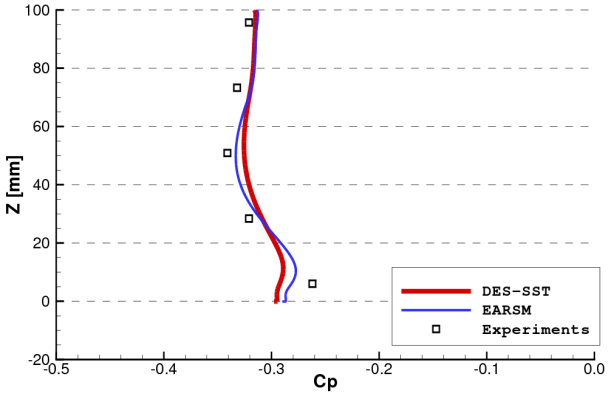

FIGURE 22. PRESSURE COEFFICIENT ON THE CAB BASE IN THE SYMMETRY PLANE.

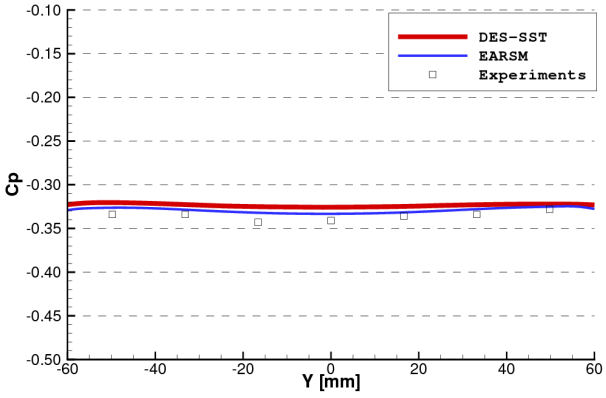

FIGURE 23. PRESSURE COEFFICIENT ON THE CAB BASE IN A PLANE AT Z = 50.9 MM.

in Figs. 25 and 26. CFD predictions and the experiment give the same pattern of pressure distribution. A small difference exists at the bottom of the outside surface of the tailgate. We can notice that the pressure on the inside surface of the tailgate is lower than on the outside surface. This indicates that the force acting on the tailgate is in the forward direction and then reducing the drag of the pickup truck. This has been demonstrated by Cooper [22] who suggests to keep the tailgate up.

The pressure coefficient distribution on the underbody, along the symmetry plane, is shown in Fig. 27. The pressure coefficient varies slightly with two local minima which correspond to the location of the wheels. This variation is attributed to the local acceleration of the underbody flow due to the reduced flow cross section area at the wheels. Numerically, we find these two local minima of pressure but at the level of the front wheels, the value is underestimated.

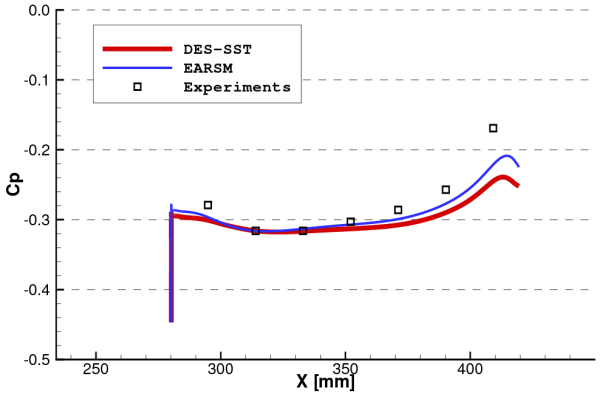

FIGURE 24. PRESSURE COEFFICIENT ON THE BED FLOOR IN THE SYMMETRY PLANE.

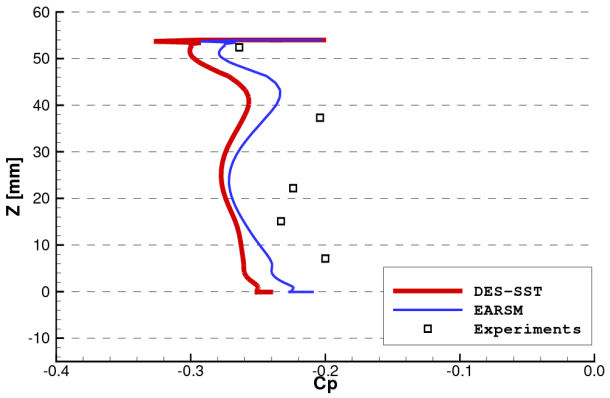

FIGURE 25. PRESSURE COEFFICIENT ON THE INSIDE SURFACE OF THE TAILGATE IN THE SYMMETRY PLANE.

Force coefficients

Table 1 shows the experimental and computed drag coefficient, Cd, and the lift coefficient Cl. For both simulations, the drag coefficient is very similar and the computed drag coefficients are overestimated 4.5% and 5.1% of the measurement for the EARSM turbulence model and the DES, respectively. However, these values are in better agreement that those presented by Khalighi [7] using two commercial CFD codes. For the lift coefficient, the numerical simulations give again the same results and underestimate the experimental value. This result is not very surprising. During, the SAE 2010 World Congress, an open discussion was focused on the lift prediction that is less successful than drag prediction. And the conclusions were that it may come from experimental measurements or the flow under the vehicle is not simulated correctly.

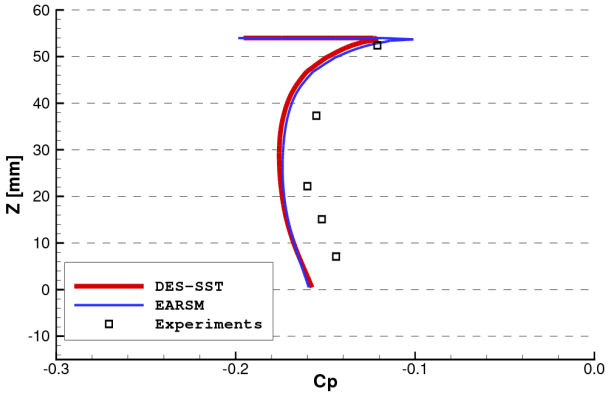

FIGURE 26. PRESSURE COEFFICIENT ON THE OUTSIDE SURFACE OF THE TAILGATE IN THE SYMMETRY PLANE.

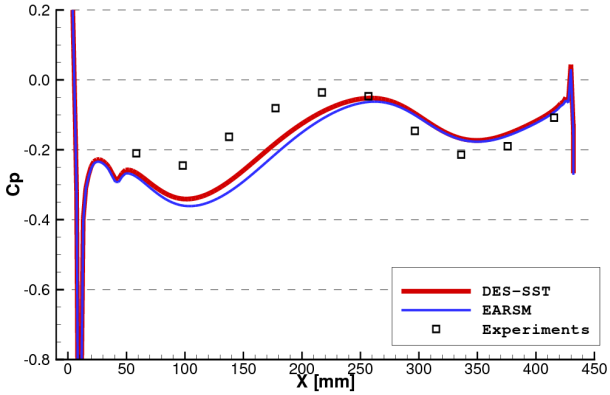

FIGURE 27. PRESSURE COEFFICIENT ON THE UNDERBODY IN THE SYMMETRY PLANE.

TABLE 1. FORCE COEFFICIENTS.

Force	EARSM	DES-SST	Experiments
Cd	0.369	0.371	0.353
Cl	0.291	0.298	0.425

CONCLUSION

This paper presents numerical simulations of the flow around a generic pickup truck. Simulations are performed using Reynolds-averaged Navier-Stokes equations by the ISIS-CFD flow solver. The objective of this paper was to assess the capabilities of CFD approach when it is applied to flow around pickup truck. Two turbulence models are used in this study: the EARSM turbulence model and a DES approach.

The comparisons between the numerical results and the experimental data show that the the structure of the flow field around the pickup truck can be well described by the ISIS-CFD flow solver. The DES approach is not more beneficial than the simulation with the EARSM turbulence model for the flow aound a pickup truck as to the distribution of pressure, average velocity and force coefficients.

It seems that the DES-SST approach is not necessary for the simulation of the flow around a pickup truck because this approach requires more CPU time than that of a simulation with the EARSM turbulence model. However, it may be interesting to try other DES approaches to see if forces are better predicted.

The objective of this paper was to compare a numerical solution with experimental data. For a full-scale pickup truck, the Reynolds number used in this study corresponds to a velocity U_{in} = 9 km/h. Consequently, a study of scale effects could be interesting.

ACKNOWLEDGMENT

The author would like to thank B. Khalighi of General Motors for placing the geometry and experimental data at its disposal. This work was granted access to the HPC resources of CINES and IDRIS under the allocation 2010 - x2010020129 made by GENCI (Grand Equipement National de Calcul Intensif).

REFERENCES

[1] Hucho, W. H., 1998. *Aerodynamics of road vehicles*. SAE International.

[2] Le Good, G. M., and Garry, K. P., 2004. On the use of reference models in automotive aeorodynamics. SAE Paper 2004-01-1308.

[3] Ahmed, S. R., Ramm, G., and Faltin, G., 1984. Some salient features of the time-averaged ground vehicle wake. SAE Paper 840300.

[4] Al-Garni, A. M., Bernal, L. P., and Khalighi, B., 2003. Experimental investigation of the near wake of a pick-up truck. SAE Paper 2003-01-0651.

[5] Lokhande, B., Sovani, S., and Khalighi, B., 2003. Transient simulation of the flow field around a pickup truck. SAE Paper 2003-01-1313.

[6] Yang, Z., and Khalighi, B., 2005. CFD simulations for flow over pickup trucks. SAE Paper 2005-01-0547.

[7] Khalighi, B., 2008. Comparison between the conventional body-fitted and the Lattice Boltzmann CFD methods for the flow around a generic pickup truck. SAE Paper 2008-01-0323.

[8] Guilmineau, E., 2008. Computational study of flow around a simplified car body. Journal of Wind Engineering and Industrial Aerodynamics.

[9] Guilmineau, E., and Chometon, F., 2009. "Effect of side wind on a simplified car model: Experimental and numerical analysis". *Journal of Fluids Enginnering,* ***31***(2).

[10] Visonneau, M., Queutey, P., and Deng, G. B., 2006. Computation of model and full-scale free-surface flows around fully-appended ships with an unstructured RANSE solver. 26th ONR Symposium on Naval Hydrodynamics, Rome.

[11] Deng, G. B., Queutey, P., and Visonneau, M., 2008. "Effet d'échelle pour des écoulements turbulent autour de dragues". *European Journal of Environmental and Civil Engineering,* ***12***(5), pp. 485–496.

[12] Guilmineau, E., Chikhaoui, O., Deng, G. B., and Visonneau, M., 2009. "Effet de vent latéral sur un modèle simplifié de voiture par une méthode DES". *Mécanique & Industries,* ***10***, pp. 203–209.

[13] Jasak, H., Weller, H., and Gosman, A., 1999. "High resolution nvd differencing scheme for arbitrarily unstructured meshes". *International Journal for Numerical Methods in Fluids,* ***31***, pp. 431–449.

[14] Rumsey, C. L., and Gatski, T. B., 2001. "Recent turbulence model advances applied to multielement airfoil computations". *Journal of Aircraft,* ***38***(5), pp. 904–910.

[15] Speziale, C. G., Sarkar, S., and Gatski, T. B., 1991. "Modeling the pressure-strain correlation of turbulence: An invariant dynamical systems approach". *Journal of Fluids Mechanics,* ***227***, pp. 245–272.

[16] Menter, F. R., 1993. "Zonal two-equation $k-\omega$ turbulence models for aerodynamic flows". In AIAA 24th Fluid Dynamics Conference, AIAA Paper 93-2906.

[17] Menter, F. R., and Kuntz, M., 2004. "Adaptation of eddy-viscosity turbulence models to unsteady separated flow behind vehicles". In *Lectures Notes in Applied and Computational Mechanics - The Aerodynamics of Heavy Vehicles: Trucks, Buses and Trains*, F. B. R. McCallen and J. Ross, eds., Vol. 19. Springer-Verlag, pp. 339–352.

[18] Strelets, M., 2001. Detached eddy simulation of massively separated flows. AIAA Paper 2001-0879.

[19] Howard, R. J. A., and Pourquie, M., 2001. "Large eddy simulation on the ahmed reference model". *Journal of Turbulence,* ***3***(1).

[20] Krajnovic, S., and Davidson, L., 2005. "Flow around a simplified car - part 1: Large eddy simulation". *Journal of Fluids Engineering,* ***127***, pp. 907–918.

[21] Al-Garni, A. M., and Bernal, L. P., 2010. "Experimental study of a pickup truck near wake". *Journal of Wind Engineering and Industrial Aerodynamics,* ***98***, pp. 100–112.

[22] Cooper, K. R., 2004. Pickup truck aerodynamics - keep your tailgate up. SAE Paper 2004-01-1146.